Time Course and Site(s) of Cytochrome *c* Tyrosine Nitration by Peroxynitrite†

Carlos Batthyány,‡,§ José M. Souza,‡ Rosario Durán,§ Adriana Cassina,‡ Carlos Cerveñansky,§ and Rafael Radi*,‡

Departamento de Bioquímica and Center for Free Radical and Biomedical Research, Facultad de Medicina, Universidad de la República, Montevideo, Uruguay, and Unidad de Bioquímica Analítica, Instituto de Investigaciones Biológicas Clemente Estable, Montevideo, Uruguay

Received December 3, 2004; Revised Manuscript Received April 12, 2005

ABSTRACT: Cytochrome *c*-dependent electron transfer and apoptosome activation require protein−protein binding, which are mainly directed by conformational and specific electrostatic interactions. Cytochrome *c* contains four highly conserved tyrosine residues, one internal (Tyr67), one intermediate (Tyr48), and two more accessible to the solvent (Tyr74 and Tyr97). Tyrosine nitration by biologically-relevant intermediates could influence cytochrome *c* structure and function. Herein, we analyzed the time course and site(s) of tyrosine nitration in horse cytochrome *c* by fluxes of peroxynitrite. Also, a method of purifying each (nitrated) cytochrome *c* product by cation-exchange HPLC was developed. A flux of peroxynitrite caused the time-dependent formation of different nitrated species, all less positively charged than the native form. At low accumulated doses of peroxynitrite, the main products were two mononitrated cytochrome *c* species at Tyr97 and Tyr74, as shown by peptide mapping and mass spectrometry analysis. At higher doses, all tyrosine residues in cytochrome *c* were nitrated, including dinitrated (i.e., Tyr97 and Tyr67 or Tyr74 and Tyr67) and trinitrated (i.e., Tyr97, Tyr74, and Tyr67) forms of the protein, with Tyr67 well represented in dinitrated species and Tyr48 being the least prone to nitration. All mono-, di-, and trinitrated cytochrome *c* species displayed an increased peroxidase activity. Nitrated cytochrome *c* in Tyr74 and Tyr67, and to a lesser extent in Tyr97, was unable to restore the respiratory function of cytochrome *c*-depleted mitochondria. The nitration pattern of cytochrome *c* in the presence of tetranitromethane (TNM) was comparable to that obtained with peroxynitrite, but with an increased relative nitration yield at Tyr67. The use of purified and well-characterized mono- and dinitrated cytochrome *c* species allows us to study the influence of nitration of specific tyrosines in cytochrome *c* functions. Moreover, identification of cytochrome *c* nitration sites in vivo may assist in unraveling the chemical nature of proximal reactive nitrogen species.

Cytochrome *c* is a small globular protein localized in the intermembrane space of mitochondria, where it participates as a redox partner in mitochondrial electron transport (*1*). In addition, when released to the cytosol, it is involved in the apoptosis pathway (*2*). Binding and interaction of cytochrome *c* with other proteins are largely directed by electrostatic forces; e.g., the association of this positively charged protein (pI ∼10) with negatively charged interfaces is a relevant known phenomenon (*3*). Post-translational modifications in cytochrome *c* can generate a change in the global or local charge distribution and may be associated with significant functional consequences (*4*, *5*). In this regard, nitration of tyrosine residues may have a strong influence on cytochrome *c* structure and function (*6*, *7*).

Peroxynitrite ($ONOO^-$/ONOOH,[1] $pK_a = 6.8$) is a strong oxidant and nitrating agent, produced in vivo after the diffusion-controlled reaction between nitric oxide and superoxide, and affects mitochondrial homeostasis. Indeed, peroxynitrite can diffuse from extramitochondrial compartments into the mitochondria or be formed in situ, where it undergoes direct and free radical-dependent target molecule reactions (*8*). At the molecular level, the predominant outcomes of peroxynitrite reactions in vivo are one- or two-electron oxidations and nitrations (*9*). The presence of protein 3-nitrotyrosine in cell cultures and tissues has been often considered a marker of peroxynitrite production, although 3-nitrotyrosine is not solely a product of peroxynitrite (*10*, *11*).

Addition of a nitro ($-NO_2$) group to tyrosine lowers the pK_a of its phenolic hydroxyl group by 2−3 units and adds a bulky moiety (*12*). When nitration takes place in relevant tyrosines, it may alter protein function and conformation.

† This work was supported by grants from Fondo Clemente Estable (CONICYT, Uruguay), Fogarty-NIH, and The Howard Hughes Medical Institute to R.R. and Third World Academy of Science to J.M.S.

* To whom correspondence should be addressed: Departamento de Bioquímica, Facultad de Medicina, Universidad de la República, Avenida General Flores 2125, CP 11800, Montevideo, Uruguay. Telephone: +598-2-9249561. Fax: +598-2-9249563. E-mail: rradi@fmed.edu.uy.

‡ Universidad de la República.

§ Instituto de Investigaciones Biológicas Clemente Estable.

[1] Abbreviations: ABTS, 2,2-azinobis(3-ethylbenzthiozoline-6-sulfonic acid) diammonium salt; ACN, acetonitrile; cytochrome c^{2+}, ferrous cytochrome; cytochrome c^{3+}, ferric cytochrome; DTPA, diethylenetriaminepentaenoic acid; ECL, luminol-enhanced chemiluminescence; HPLC, high-pressure liquid chromatography; KCl, potassium chloride; KCN, potassium cyanide; MALDI-TOF, matrix-assisted laser desorption ionization time of flight; MS, mass spectrometry; $ONOO^-$/ONOOH, peroxynitrite; RP-HPLC, reverse-phase high-pressure liquid chromatography; SDS, sodium dodecyl sulfate; TNM, tetranitromethane; TFA, trifluoroacetic acid; Tris, tris(hydroxymethyl)aminomethane.

10.1021/bi0474620 CCC: $30.25
Published on Web 05/12/2005

Nitrated and inactivated MnSOD is found in acute and chronic inflammatory processes in both animal models and human diseases (*13*, *14*), being a prime example of the loss of enzyme activity associated with nitration. Alternatively, tyrosine nitration may induce a "gain of function", in which case a small fraction of nitrated protein can elicit a substantive biological signal (*15*). This attractive concept has been demonstrated for a few proteins such as cytochrome *c*, which acquires a strong peroxidase activity after nitration (*7*), and nitrated fibrinogen, which accelerates clot formation (*16*). Additionally, increased levels of tissue protein 3-nitrotyrosine may serve as potential autoantigens (*17*).

Cytochrome *c* is present at high concentrations in the intermembrane space (>1 mM) (*18*), thus being a potential relevant target of peroxynitrite in mitochondria (*7*). Reduced cytochrome *c* (ferrous or cytochrome c^{2+}) undergoes a direct one-electron oxidation by peroxynitrite ($k = 2.5 \times 10^4$ M^{-1} s^{-1}) (*19*), while ferric cytochrome *c* (oxidized cytochrome *c* or cytochrome c^{3+}) is nitrated by reactions with peroxynitrite-derived radicals (*7*). Moreover, in the presence of H_2O_2, cytochrome *c* can be also nitrated by nitrite (*20*) or •NO (*21*) via peroxynitrite-independent mechanisms. Different observations indicate that excess mitochondrial reactive nitrogen intermediates lead to the nitration and release of cytochrome *c* (*22*, *23*), and nitrated cytochrome c^{3+} has already been detected in vivo (*24*).

Cytochrome *c* nitration by peroxynitrite (*7*) and tetranitromethane (TNM) has been previously studied (*6*, *25*). Indeed, early work indicated that exposure to an excess of TNM resulted in tyrosine nitration (mainly at Tyr67), and this was accompanied by changes in cytochrome *c* physicochemical properties and respiratory function (*6*, *25*). Similarly, peroxynitrite caused nitration of cytochrome *c*, leading to a dose-dependent loss of Met80−heme iron interactions and an increase in peroxidase activity and making the protein resistant to reduction by ascorbate (*7*). Additionally, peroxynitrite-treated cytochrome *c* loses its electron transport capacity in the mitochondrial inner membrane (*7*).

In our previous work, a 10-fold excess of peroxynitrite over the protein induced formation of mono-, di-, and trinitrated species (*7*), but mass spectrometry analysis just allowed the identification of two nitration sites, namely, at Tyr67 and Tyr48 (*7*). During these studies, nitration sites were assessed on a cytochrome *c* treated with a high initial concentration of peroxynitrite, and the whole mixture was digested and analyzed without previous purification of the main nitrated products. Moreover, due to the presence of remaining unmodified cytochrome *c* after peroxynitrite treatment, the approach limited the conclusions concerning the functional consequences of cytochrome *c* nitration (*7*).

Herein, we further characterized the nitration of cytochrome *c* by (a) utilizing physiologically-relevant fluxes of peroxynitrite in the absence and presence of carbon dioxide and (b) applying a different analytical strategy, through the initial purification of the main reaction products, subsequent study of the nitration site(s), and the functional consequences of each specific modification. This approach revealed preferential sites of tyrosine nitration of cytochrome *c* by peroxynitrite and also disclosed the influence that each nitrated tyrosine had on specific functional properties of cytochrome *c*.

EXPERIMENTAL PROCEDURES

Chemicals. Horse heart cytochrome *c* (C-7752) was obtained from Sigma. This cytochrome *c* preparation was selected because it is purified without the use of trichloroacetic acid, which otherwise leads to substantial amounts of deamidated and polymeric forms (*26*). The purity of the cytochrome *c* preparation used herein was >95% as determined by chromatographic, spectroscopic, electrophoretic, and mass spectrometric criteria. 2,2-Azinobis(3-ethylbenzthiozoline-6-sulfonic acid) diammonium salt (ABTS), diethylenetriaminepentaenoic acid (DTPA), and horseradish peroxidase were also obtained from Sigma. Sequencing grade modified trypsin was obtained from Promega. Tetranitromethane (TNM) was obtained from Fluka, and hydrogen peroxide was obtained from Baker. All other reagents were analytical-grade. Rabbit polyclonal antibody raised against protein 3-nitrotyrosine was purified in our laboratory as described elsewhere (*27*). Peroxynitrite was synthesized, quantitated, and handled as previously described (*28*).

Cytochrome c Nitration. Nitration of cytochrome c^{3+} was performed by reaction with either peroxynitrite or TNM. Peroxynitrite was added to cytochrome c^{3+} (200 μM or 1 mM) in 200 mM potassium phosphate and 100 μM DTPA at pH 7.0 and 25 °C as a bolus (2 mM, 10-fold excess over cytochrome *c*) or as a continuous flux (0.13 mM min^{-1}) using a motor-driven syringe (SAGE Instruments, Boston, MA) as described previously (*29*), under vigorous vortexing or stirring, respectively, to circumvent mixing artifacts. The pH was controlled at the end of the reaction and was always below 7.4. In some experiments, $NaHCO_3$ (25 mM) was added, to test the effect of carbon dioxide (in equilibrium with bicarbonate) that plays a modulatory role in peroxynitrite-dependent nitration reactions in vivo because of the intermediate formation of carbonate and nitrogen dioxide radicals (*15*). TNM (40 mM) was added to cytochrome c^{3+} (1 mM) in 0.1 M Tris-HCl and 0.1 M KCl (pH 8.0) at room temperature, and the reaction was followed for up to 30 min. The reaction was stopped by passing the mixture through a desalting column (HiTrap, 5 mL, Amersham Biosciences) equilibrated with 0.1 M Tris-HCl and 0.1 M KCl (pH 8.0).

Biochemical Analyses. Peroxidase activity was assayed with 1.3 mM ABTS and 1.2 mM H_2O_2 at 20 °C with the addition of native or nitrated cytochrome *c* (0.6 μM) in 100 mM potassium phosphate and 100 μM DTPA (pH 7.2). ABTS oxidation was followed at 420 nm [$\epsilon = 36$ mM^{-1} cm^{-1} (*30*)]. All kinetic measurements were performed and absorption spectra recorded in a Shimadzu UV-2401 PC spectrophotometer. Protein concentrations were determined by the bicinchoninic acid (BCA) method (*31*).

HPLC Purification of Cytochrome c Nitration Products. Reaction mixtures after treatment of cytochrome *c* with peroxynitrite or TNM were analyzed at different times by cation-exchange HPLC using a sulfopropyl-TSK column (7.5 mm × 75 mm; Tosoh Biosep). The flow rate was 0.7 mL min^{-1}, and the column was equilibrated with 10 mM ammonium acetate (pH 9.0). Products were separated using a linear gradient of ammonium acetate (pH 9.0) from 10 to 400 mM over the course of 50 min.

Tryptic Digestion and Peptide Mapping. Cytochrome c^{3+} samples (control and peroxynitrite-treated) previously purified by cation-exchange HPLC were lyophilized and resus-

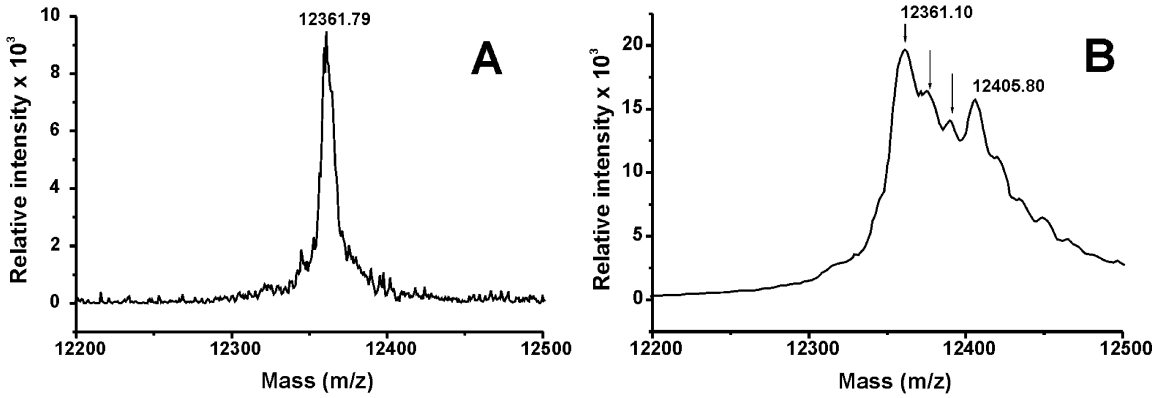

FIGURE 1: MALDI-TOF mass spectrum of native (A) and peroxynitrite-treated (B) cytochrome *c*. Cytochrome *c* (200 μM) in 200 mM potassium phosphate buffer and 100 μM DTPA (pH 7.0) was subjected to a bolus addition of peroxynitrite (2 mM).

pended in 100 mM ammonium bicarbonate (pH 8.3). Cleavage was carried out with sequencing-grade modified trypsin in a 1:100 ratio (w/w) at 37 °C for 16 h. Peptides were separated and purified by RP-HPLC (LKB binary system) using an octadecyl-silica gel reverse-phase column (5 μm, 2.1 mm × 150 mm, 300 Å, Vydac) with UV detection. Solvent A was 0.1% trifluoroacetic acid, and solvent B was 0.07% trifluoroacetic acid in acetonitrile. Peptides were eluted using an increasing linear gradient of solvent B from 0 to 45% in 90 min with a flow rate of 0.25 mL/min and spetrophotometric detection at 220 and 365 nm. All peptide fractions in control, peroxynitrite-treated, and TNM-treated cytochrome c^{3+} were collected manually and submitted for molecular mass determination.

Mass Spectrometry Studies. MALDI-TOF-MS was carried out in a Voyager DE PRO system (Applied Biosystems, Foster City, CA), equipped with a N_2 laser source ($\lambda = 337$ nm). Mass spectra were acquired for positive ions in the linear and reflector modes. For whole molecular mass determinations, 10 μL of native, peroxynitrite-treated, or TNM-treated cytochrome *c* (200 μM) was mixed with 5 μL of reverse-phase Poros R2 suspension and the mixture stirred for 10 min at room temperature. After centrifugation, the pellet was washed with 0.1% TFA (3 × 100 μL). Proteins were eluted by adding the matrix solution [sinapinic acid, 10 mg/mL in 50% acetonitrile (ACN), 0.2% TFA]. After centrifugation, the supernatant was applied to the stainless steel sample plate. Similarly, peptides from RP-HPLC fractions were concentrated under a nitrogen stream and analyzed by MALDI-TOF-MS using α-cyano-4-hydroxycinnamic acid as the matrix. Peptide masses were measured in the reflector mode with an accuracy close to 50 ppm attained with internal mass calibration using characteristic cytochrome *c* tryptic peptides as mass standards.

Electrophoretic Analysis. Samples of control, TNM-treated, and peroxynitrite-treated cytochrome *c* were separated by electrophoresis on SDS−15% polyacrylamide gels and analyzed after blotting (20 mA, 16 h) to nitrocellulose membranes (pore size, 0.45 mm; Hybond-C extra; Amersham). Nonspecific binding sites were blocked for 1 h with 5% bovine serum albumin, 50 mM Tris-HCl, 150 mM NaCl, and 0.6% Tween 20 (pH 7.4). Nitrocellulose membranes were probed with rabbit polyclonal antibody against nitrotyrosine (1:1000 dilution) in blocking buffer for 1 h (*27*). After being extensively washed in 50 mM Tris-HCl, 150 mM NaCl, and 0.6% Tween 20 (pH 7.4), the immunocomplexed membranes were further incubated (1 h) with 1:6000 horseradish peroxidase-conjugated donkey polyclonal anti-rabbit IgG antibodies. Probed membranes were washed in blocking buffer containing 0.3% Tween 20, and the immunoreactive protein was detected by luminol-enhanced chemiluminescence (ECL, Amersham).

Mitochondrial Preparation and Respiration Assay. Intact rat heart mitochondria isolation and cytochrome *c* extraction were carried out as described previously (*7*). The respiratory control ratio for complex II-dependent respiration was evaluated with succinate (5 mM) and typically ranged between 3 and 5. The concentration of cytochrome *c* was determined by measuring the absorbance at 410 nm [$\epsilon = 106$ mM^{-1} cm^{-1} (*32*)]. Typically, 0.7 ± 0.1 nmol of cytochrome *c* per milligram of mitochondrial protein was extracted. When the sample was replenished with either native or nitrated cytochrome *c*, the same amount was supplemented. Oxygen consumption was assessed in a 1.6 mL water-jacketed chamber using a Clark electrode as previously described (*7*).

RESULTS

Peroxynitrite-Mediated Cytochrome c Modification and Nitration. Cytochrome *c* (200 μM) was subjected to bolus addition of peroxynitrite (2 mM). The half-life of peroxynitrite under these experimental conditions is ~3 s, and therefore, the reaction was completed in less than 30 s (*9*). The treatment resulted in the generation of at least one product differing by 45 Da from the parent protein (mass shift from 12 361.1 to 12 405.8 Da; see panels A and B of Figure 1), consistent with the addition of one nitro group per molecule of cytochrome *c*. Moreover, mass signals at 12 389 and 12 373 Da were also detected (see Figure 1B, arrows), in agreement with the fragmentation pattern observed when nitrated molecules are analyzed by MALDI-TOF (*33*).

Time Course of Peroxynitrite-Mediated Cytochrome c Nitration. According to the protocol described above, it is not possible to take samples at different time points. Thus, to follow the time course of cytochrome *c* nitration under conditions that more closely mimic a sustained exposure to steady-state levels of peroxynitrite, cytochrome *c* (1 mM) was treated with an infusion of peroxynitrite (0.13 mM min^{-1}). The ease with which cytochrome *c* can be chro-

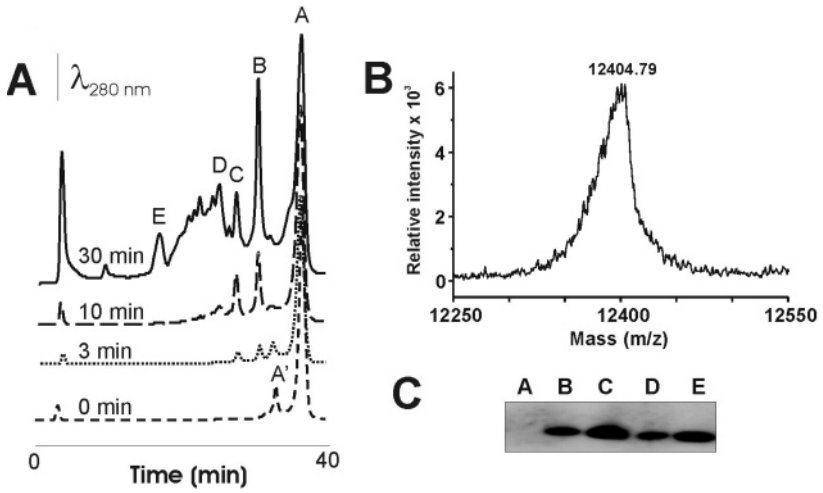

FIGURE 2: Time course of peroxynitrite-mediated cytochrome *c* modification. Cation-exchange HPLC purification and analysis of products by MALDI-TOF and immunochemistry. Cytochrome *c* (1 mM) in 200 mM potassium phosphate buffer and 100 μM DTPA (pH 7.0) was treated with an infusion of peroxynitrite (0.13 mM min^{-1}). (A) The reaction mixture (600 μg of protein) was analyzed at different time points by cation-exchange HPLC. (B) MALDI-TOF mass spectrum of an early product (peak B in panel A), with a mass increased by 45 Da compared to that of the native protein (the same result was obtained for peak C in panel A; data not shown). (C) Western blot analysis of the main products of peroxynitrite-treated cytochrome *c*. Five micrograms of each fraction in panel A was run on a SDS−15% PAGE gel and examined by Western blot analysis using an anti-nitro-Tyr antibody.

Table 1: Molecular Masses of Peroxynitrite-Treated Cytochrome *c* Products Obtained from Cation-Exchange HPLC Shown in Figure 2

peak	molecular mass (Da)	assignment
A	12 361	native cytochrome c^{3+}
A′	12 361	native cytochrome c^{2+}
B	12 406	mononitrated
C	12 405	mononitrated
D	12 452	dinitrated
E	12 495	trinitrated

matographed on cation exchangers and the extreme sensitivity of the chromatographic behavior to changes in charge distribution at the molecular surface and/or net charge (*1*) prompted us to analyze the reaction mixture by cation-exchange HPLC. This approach allowed us not only to easily separate the two redox forms of cytochrome *c* (i.e., ferric and ferrous cytochrome *c*) present in commercial preparations but also to separate different species displaying less positive net charge (Figure 2A) that were time-dependently formed during the infusion of peroxynitrite. Early reaction products (peaks B and C) showed an increase of 45 Da in molecular mass, compatible with the addition of a nitro group per molecule (Table 1 and Figure 2B). Products with a shift of 90 Da (Figure 2, peak D, and Table 1) and 135 Da (Figure 2, peak E, and Table 1) were also formed but at higher doses of peroxynitrite (longer infusion times), suggesting the formation of di- and trinitrated derivatives. Importantly, the decrease in the amount of native form (peaks A and A′, Figure 2) correlated almost quantitatively with the increase in the levels of the nitrated forms over time (peaks B−E, Figure 2). For example, after peroxynitrite infusion for 30 min, 205 μg out of 600 μg of total cytochrome *c* protein injected into the HPLC system was present as cytochrome c^{3+} (peak A), with the rest mainly evolving to mono-, di-, and trinitrated forms (161, 52, 51, and 66 μg in peaks B−E, respectively). Main products of the reaction were also analyzed immunochemically using a previously characterized anti-nitro-Tyr antibody (*27*) (peaks B−E, Figure 2C), and confirmed that each of the products was nitrated.

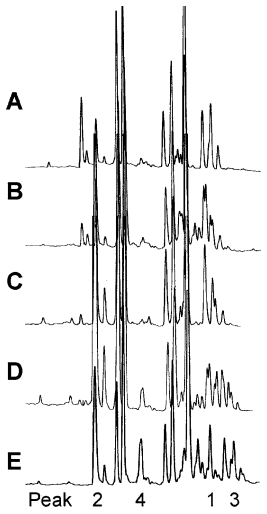

FIGURE 3: RP-HPLC separation of trypsin-digested native and peroxynitrite-treated cytochrome *c*. Each of the main products collected from the cation-exchange chromatography (peaks A−E in Figure 2) were desalted and digested with trypsin in 0.1 M NH_4HCO_3 (pH 8.3) for 24 h at 20 °C. Digestion mixtures of peaks A−E were analyzed by RP-HPLC with UV detection at 220 nm (shown in the figure) and 365 nm (not shown). All peptides were collected manually and their masses measured by MALDI-TOF. Labeled peaks also absorb at 365 nm.

Identification of Cytochrome c Nitration Sites after Reaction with Peroxynitrite. Each main product collected from cation-exchange chromatography (Figure 2, peaks A−E) was desalted and digested with trypsin before being analyzed and separated by RP-HPLC (Figure 3). Peptide mapping of each product was different from that of the native protein (B−E vs A). The presence of new peptides also absorbing at 365 nm (numbered peaks in Figure 3, not shown) was compatible with the formation of nitrotyrosine-containing products (*34*). HPLC peptide fractions were analyzed by MALDI-TOF-MS. The mass spectrum of peptide 1, the 365 nm-absorbing peptide identified in the tryptic digestion of the main mononitrated cytochrome *c* species (Figure 3B), exhibited a mass signal of 1009.2 Da (Figure 4 and Table 2) that could

Table 2: Monoisotopic Molecular Masses of Nitrated Peptides and Identification of Nitration Sites by Post-Source Decay Analysis

peptide	theoretical mass (Da) [(M + H)$^+$]	theoretical mass + 45[a] (Da) [(M + H)$^+$]	observed masses (Da)	assigned sequence	nitrated tyrosine
			1009.22		
1	964.53	1009.53	993.23	^{92}EDLIA^{97}**Y**LK^{99}	Y97
			978.00		
			723.13		
2	678.37	723.37	707.14	^{74}**Y**IPGTK^{79}	Y74
			691.15		
			1668.77		
3	1623.79	1668.79	1652.77	^{61}EETLME^{67}**Y**LENPKK^{73}	Y67
			1636.77		
			1643.93		
4	1598.79	1643.79	1627.94	^{39}KTGQAPGFT^{48}**Y**TDANK^{53}	Y48
			1611.94		

[a] Addition of a nitro ($-NO_2$) group results in a molecular mass increase of 45 Da.

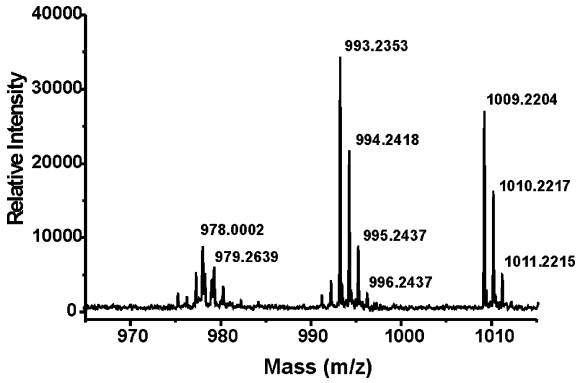

FIGURE 4: Mass spectrum of a nitrated peptide. Peptides were purified by RP-HPLC and analyzed by MALDI-TOF-MS. Herein, as an example, is shown the mass spectrum of peptide 1 (Figure 3B) obtained in the positive reflector mode using α-cyano-4-hydroxycinnamic acid as the matrix. The sequence corresponds to ^{92}EDLIA-NO_2-^{97}YL^{99}K.

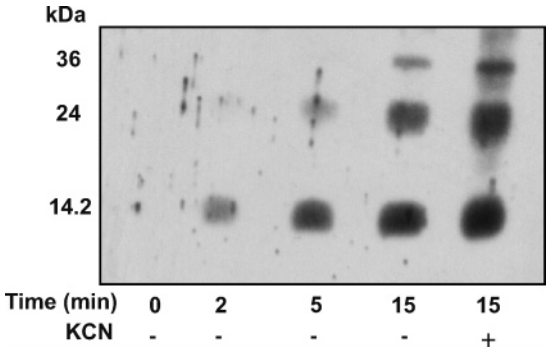

FIGURE 5: Immunochemical analysis of TNM-treated cytochome *c* nitration. Cytochrome *c* (1 mM) in 100 mM Tris-HCl (pH 8.0), 100 mM KCl, or KCN was treated with 40 mM TNM. After 0, 2, 5, and 15 min, samples were taken and the reaction was taken to completion by passing the mixture through a Hi-Trap desalting column. Five micrograms of each sample was run on a SDS−15% PAGE gel and examined by Western blot analysis against anti-nitro-Tyr.

be assigned to peptide ^{92}EDLIA^{97}YLK^{99} plus 45 Da. In addition, a fragmentation pattern characteristic of nitropeptides was also observed (*33*). The same triplet of peaks was observed in all peptides with absorbance at 365 nm (peptides 2−4 in Figure 3; also see Table 2). Post-source decay sequencing by mass spectrometry confirmed a tyrosine residue as the nitration site (Table 2). In the other mononitrated cytochrome *c* species (peak C, Figure 2A), a different nitrated peptide was identified (peptide 2 in Figure 3C) corresponding to the ^{74}YIPGTK^{79} peptide. Thus, at least two different mononitrated cytochrome *c* species were formed at low doses of peroxynitrite: nitro-Tyr97 and nitro-Tyr74 cytochrome *c*. On the other hand, when we analyzed the di- and trinitrated species (peaks D and E in Figure 2), three and four different tyrosine-containing nitrated peptides were found, indicating that all four tyrosine residues were nitrated by peroxynitrite in different dinitrated (i.e., Tyr97 and Tyr67 or Tyr74 and Tyr67) and trinitrated (i.e., Tyr97, Tyr74, and Tyr67) products. While nitrotyrosine 67 was well represented in dinitrated species, nitrotyrosine 48 was primarily contained in trinitrated forms of cytochrome *c* only (peptide 4 in Figure 3E and Table 2). Importantly, at the cytochrome *c* and peroxynitrite concentrations that were utilized, the nitration pattern was similar when 25 mM bicarbonate was added (not shown), in line with the comparable extents of peroxynitrite-dependent cytochrome *c* nitration and spectroscopic changes reported before the modulatory action of carbon dioxide had been evaluated (*7*). To note, at high peroxynitrite concentrations (>4 mM total dose), small amounts of nitro-Trp59 were also found, consistent with the possibility of tryptophan nitration by peroxynitrite (*35*).

Cytochrome c Nitration by TNM and the Effect of Cyanide. Cytochrome *c* (1 mM) in the absence or presence of potassium cyanide (100 mM) was treated with TNM (40 mM). Samples were taken at different reaction times and analyzed by Western blotting against anti-nitro-Tyr. A time-dependent level of nitration was observed, but surprisingly, potassium cyanide increased TNM-dependent cytochrome *c* nitration (Figure 5). To further characterize nitration of cytochrome *c* (1 mM) by TNM, early reaction products (5 min) were separated and purified by cation-exchange HPLC (Figure 6, panel I, peaks B−D). After desalting, the fractions were digested with trypsin and subjected to analysis by RP-HPLC (Figure 6, small panels). Peptides were collected manually and studied by MALDI-TOF-MS (see Table 2). Main reaction products of cytochrome *c* treated with TNM for 5 min were identified as two different mononitrated cytochrome *c* species (peak C in Tyr74 and peak B in Tyr67) as well as a single dinitrated cytochrome *c* at Tyr74 and Tyr67 simultaneously (peak D).

Functional Consequences of Cytochrome c Nitration: Peroxidase Activity and Electron Transport Capacity of Nitrated Cytochromes. To assess the functional consequences of cytochrome *c* nitration, we first analyzed the peroxidase

Table 3: Mitochondrial Electron Transport Capacity and Peroxidase Activity of Nitrated Cytochrome *c* Species

	succinate-dependent respiration[a]		peroxidase[b]	
	rate (mM O_2/min)	% of control	activity (μM/min)	% of control
native	0.071 ± 0.032	100	1.67 ± 0.11	100
NO_2-Y74	0.039 ± 0.011	55	7.69 ± 0.11	460
NO_2-Y97	0.064 ± 0.015	90	4.58 ± 0.08	274
NO_2-Y67	0.015 ± 0.011	21[c]	4.77 ± 0.12	285
di-NO_2-Y[d]	0.028 ± 0.012	39	11.72 ± 0.15	701
di-NO_2-Y (Y74−Y67)[e]	ND[f]	−	6.2 ± 0.2	371
tri-NO_2-Y[g]	ND[f]	−	12.2 ± 0.2	730
peroxynitrite-treated[h]	0.026 ± 0.013	36.6	9.35 ± 0.25	560

[a] Oxygen consumption in cytochrome *c*-depleted rat heart mitochondria (0.5 mg/mL) was assessed with the addition of 5 mM succinate and 0.7 mmol of cytochrome *c*/mg. The rate of respiration without addition of cytochrome *c* was 0.004 ± 0.001 mM O_2/min. [b] Native or nitrated cytochrome *c* (0.6 μM) in 100 mM potassium phosphate and 0.1 mM DTPA (pH 7.2) was incubated with ABTS and H_2O_2 at 20 °C. ABTS oxidation was followed at 420 nm. The Tyr67 mononitrated product was formed upon treatment of cytochrome *c* with TNM as described in the legend of Figure 6. All other species were purified from peroxynitrite infusion experiments, as described in the legend of Figure 2. [c] Data extracted from ref *6*. [d] From peroxynitrite treatment, a mix of dinitrated forms, mainly dinitro-Tyr97−Tyr67 and dinitro-Tyr74−Tyr67 (fraction D in Figure 2). [e] TNM treatment, dinitro-Tyr74−Tyr67 (fraction D in Figure 6). [f] Not determined. [g] TNM treatment, i.e., trinitro-Tyr97−Tyr74−Tyr67 (fraction E in Figure 6). [h] Data extracted from ref *7*; a mixture of nitrated and native forms.

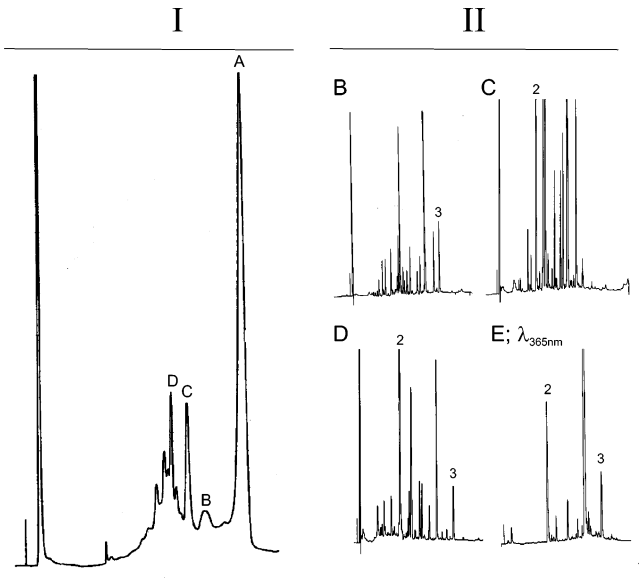

FIGURE 6: HPLC and MS analysis of TNM-treated cytochrome *c*. Cytochrome *c* (1 mM) was treated for 5 min as described in the legend of Figure 5. Reaction products were separated and purified by cation-exchange HPLC (panel I). After desalting had been carried out, the main products (peaks A−D) were digested with trypsin and the digestion mixtures analyzed by RP-HPLC with UV detection at 220 nm (B−D in panel II). Labeled peaks also absorb at 365 nm (panel E; same run as panel D but recording with 365 nm detection) and were identified by MALDI-TOF-MS (Table 2; same nomenclature as in Figure 3).

activity of the main nitrated products. Native, mononitrated, and dinitrated cytochrome *c* (0.6 μM) were incubated with ABTS and H_2O_2 at 20 °C. ABTS oxidation was followed at 420 nm. Nitration of Tyr67, Tyr74, and Tyr97 each increased peroxidase activity of cytochrome *c* by >250% (Table 3). Dinitration increased even more the peroxidase activity of the protein (Table 3), in mixed dinitrated (i.e., Tyr97 and Tyr67 or Tyr74 and Tyr67; peak D fraction in Figure 2) or singly dinitrated forms (i.e., Tyr74 and Tyr67; peak D fraction in Figure 6), suggesting an additive effect of each nitration. Moreover, trinitrated species (i.e., Tyr97, Tyr74, Tyr67) displayed increased peroxidase activity as well. Then, we assessed the function of purified nitrated cytocrome *c* species in succinate-dependent oxygen consumption of cytochrome *c*-depleted mitochondria (Table 3). Addition of nitro-Tyr74 cytochrome *c* restored respiration rates to only 55% of control values (Table 3); nitration of cytochrome *c* in Tyr97 had a less pronounced effect but still did not fully restore oxygen consumption. Moreover, dinitrated forms were even less capable of restoring the succinate-dependent oxygen consumption (Table 3) (*7*). Sokolovsky et al. (*6*) also reported decreased oxygen consumption rates in cytochrome *c*-depleted mitochondria upon addition of a cytochrome *c* in which Tyr67 was modified by nitration (Table 3).

The enhanced peroxidase activity of nitrated cytochromes is likely to be due to the breaking of the Met80 sulfur−Fe bond at the sixth coordination position of the heme, which in turn largely favors the accessibility of hydrogen peroxide to the iron atom (*7*). The integrity of the sixth coordination position can be followed at 695 nm (*36*). The loss of 695 nm absorbance in peroxynitrite-treated cytochrome *c* (*7*) and mononitrated cytochrome *c* in Tyr67 [by TNM treatment (*6*)] has been interpreted as an "early" alkaline transition (*37*) due to the decrease in pI determined by the addition of a $-NO_2$ group to tyrosine, which is known to decrease the pK_a of the phenolic −OH group from ~10 to 7.5 (*12*). Indeed, mononitrated cytochrome *c* in either Tyr97 or Tyr74 leads to a bleaching of the 695 nm absorbance band at pH 7.4, which was completely recovered at low pH, in agreement with the reversibility of the process (Figure 7). Therefore, the enhanced peroxidase activity of nitrated cytochromes *c* observed at physiological pH can be explained on the basis of the displacement of the Met80 ligand from the heme iron after tyrosine nitration.

DISCUSSION

Peroxynitrite mediates cytochrome c^{3+} tyrosine nitration in all four tyrosine residues but in a preferential order and not randomly. A flux of peroxynitrite caused the time-dependent formation of different nitrated species, all less positively charged than native cytochrome *c*. At low doses of peroxynitrite, the main reaction products were two different mononitrated cytochromes *c* at Tyr97 and Tyr74, as shown by peptide mapping and mass spectrometry analysis (Figures 2 and 3). At higher doses, all four tyrosine residues in cytochrome *c* were nitrated, included in di- and trinitrated species, with Tyr67 well represented in dinitrated species and Tyr48 being the least prone to nitration. The pattern of

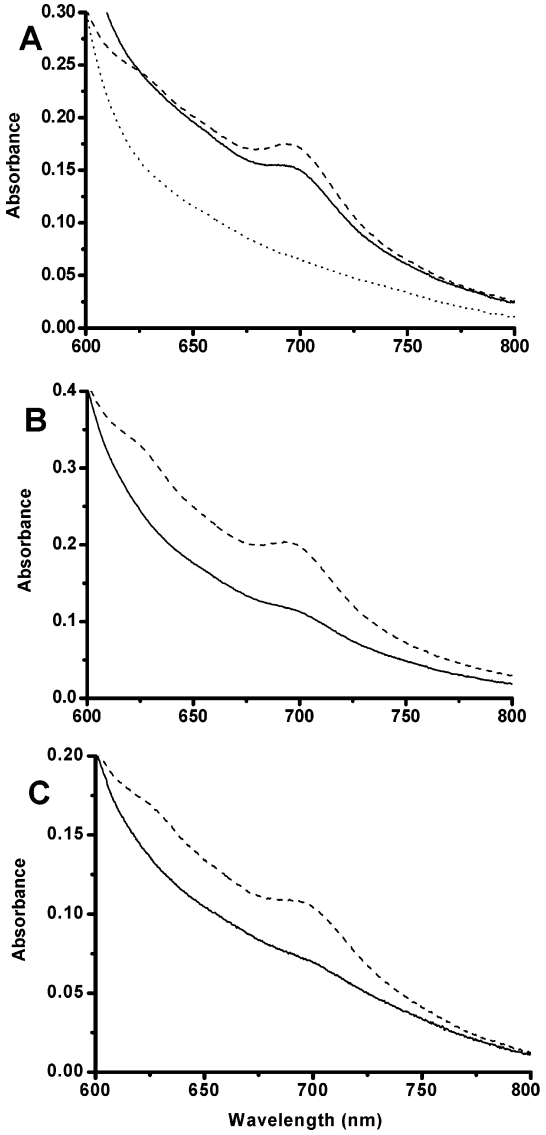

FIGURE 7: Spectral analysis of the Met80−heme bond in mononitrated cytochrome *c*. Peroxynitrite-treated cytochrome *c* was separated by cation-exchange HPLC as described in the legend of Figure 2A, and mononitrated forms of Tyr97 and Tyr74 were purified and concentrated for spectral analysis. Spectra of cytochrome *c* (0.2 mM) were recorded between 600 and 800 nm in 100 mM potassium phosphate buffer at different pHs for (A) control, (B) NO_2-Tyr97, and (C) NO_2-Tyr74 cytochrome *c* at pH 7.4 (—) and 5.0 (- - -). Given a pK_a of 9.3 for horse heart cytochrome *c* at an ionic strength of 0.1 M, the spectra of control cytochrome at pH 5.0 and 7.4 are essentially the same; thus, for control cytochrome *c*, the spectrum at pH 10 (···) is also shown to confirm the "alkaline transition" observed above pH 9.5 in native cytochrome c^{3+} due to the loss of the Met80−heme iron bond (*36*).

nitration of cytochrome *c* by TNM (Figure 6) was comparable to that obtained with peroxynitrite, but an increased relative nitration yield in Tyr67 could be observed, consistent with the earlier report (6).

Peroxynitrite-dependent tyrosine nitration is typically a free radical-mediated mechanism. In fact, the two most widely invoked mechanisms of biological nitration, namely, the peroxynitrite and the heme peroxidase pathways, lead to the concomitant formation of tyrosyl radicals and $^{\bullet}NO_2$, which combine at diffusion-controlled rates to form 3-nitrotyrosine (*15*). The oxidants leading to the tyrosyl radical are $^{\bullet}OH$, $CO_3^{\bullet-}$, or oxo−metal complexes (*15*). Because of the short

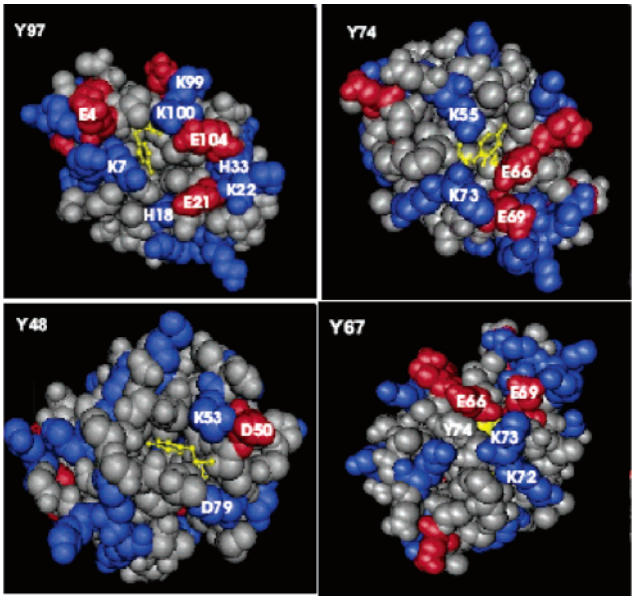

FIGURE 8: Three-dimensional structure of cytochrome *c*. In each panel, the specific tyrosine residues are colored yellow; in the Tyr67 panel (bottom right), Tyr74 can be also seen numbered in white. Negative (red) and positive (blue) charged residues localized near a tyrosine residue are also depicted. Data were taken from Protein Data Bank entry 1HRC.

half-life and reactivity of $^{\bullet}OH$, free radical-mediated tyrosine nitration generally favors nitration of solvent-accessible tyrosine residues (*38*).[2] Tyr97 and Tyr74 are clearly exposed at the surface of the protein and surrounded by charged residues (see Figure 8). Tyr67 and Tyr48 are localized more deeply in the protein core and thus in a more hydrophobic environment. Moreover, Tyr67 is almost occluded and separated from the surface by Tyr74 (Figure 8). These structural features could themselves be a rational explanation for the preferential and early nitration of Tyr97 and Tyr74 by peroxynitrite.

All mononitrated cytochromes *c* that were formed displayed increased peroxidase activity, although more pronounced for Tyr74 (Table 3). An increased peroxidase activity as a consequence of a first nitration is consistent with the loss of Met80 coordination with the sixth coordination position of the Fe atom allowing binding of H_2O_2 to the heme (*7*), in agreement with the spectral analysis performed for the mononitrated forms in Tyr67 (*6*) and in Tyr97 and Tyr74 (Figure 7). Moreover, the fact that dinitrated cytochromes *c* are formed even in the presence of excess unmodified cytochrome *c* probably points to a preferential metal center-catalyzed mechanism for the second nitration site at Tyr67, located only ~4 Å from the heme moiety.

In our previous work (*7*), the main nitrated residue that was reported was Tyr67. During those studies, we mapped nitration sites on a cytochrome *c* that was treated with high initial doses of peroxynitrite and without purification of

[2] Unless the nitration process is "site-specifically" directed by the reaction of peroxynitrite with a transition metal center (*15*) or an internal tyrosine residue behaves as a "sink" of one-electron oxidations in the protein surface by electron migration through the backbone (*39*). Metal-catalyzed nitration of the first modified tyrosine residue is ruled out as all coordination positions of the heme iron in cytochrome c^{3+} are occupied and cytochrome *c* does not accelerate peroxynitrite decomposition (*19*).

reaction products. Mononitrated cytochromes *c* (i.e., at Tyr97 and Tyr74) are consumed at higher doses of peroxynitrite, leading to dinitrated products that involve nitration of Tyr67, thus enriching the reaction mixture with nitro-Tyr67-containing peptides. Moreover, as previously shown for the proteosome-dependent protein degradation, highly modified products (i.e., di- and trinitrated proteins) could be more easily digested by trypsin (*40*). Thus, these considerations appear to account for the differences between our previous work (*7*) and this report; the more laborious methodology utilized herein undoubtedly allowed us to identify nitration sites in a more precise and thorough manner.

Previously, Sokolovsky et al. also reported nitration of cytochrome *c* by TNM, specifically at Tyr67, showing that nitrocytochrome *c* was unable to restore the respiratory function of cytochrome *c*-depleted mitochondria (*6*). In the presence of cyanide, which binds to the sixth coordination position of the heme iron, the authors reported an inhibition of nitration (*6*). Using similar experimental conditions, we found not only TNM-mediated Tyr67 but also Tyr74 nitration and formation of a single dinitrated species in Tyr74 and Tyr67 (Figure 6, panel II). Surprisingly, our results showed that cyanide enhanced TNM-mediated tyrosine nitration in cytochrome *c* (Figure 5), and the reason for the discrepancy is not evident. However, a similar nitration enhancement effect of cyanide was found by Castro et al. for peroxide- and nitrite-mediated tyrosine nitration (*20*), and it was thought to depend on the formation and reactions of cyanide-derived radicals. Indeed, cyanide-derived radicals initiate potent oxidative chemistry (see, for example, ref *41*) which may favor tyrosyl radical formation and oxidation of nitrite to nitrogen dioxide. Moreover, when cyanide is bound, cytochrome *c* no longer has its native structure which may favor nitration reactions. Nitration of Tyr74 of cytochrome *c* and to a lesser extent of Tyr97 affected oxygen consumption (Table 3).[3] Dinitrated species of cytochrome *c*, i.e., at Tyr74 and Tyr67, had an even greater alteration in electron transport capacity (Table 3), confirming that nitration in either Tyr74 or Tyr67 has profound effects on cytochrome *c* functions. In most cases, the gains in peroxidase activity of nitrated cytochrome *c* correlated well with the inhibition of mitochondrial oxygen consumption (Table 3).

Our work shows that Tyr97 is a preferential target for peroxynitrite and may contribute, in an indirect way, to an autoimmunological response by eliciting self-antigens. Indeed, in the moth pigeon cytochrome *c* peptide MCC_{88-103} which comprises a well-characterized model for the study of MHC restriction and T cell recognition, the peptide containing nitro-Tyr97 triggers T cell recognition. Conversion of this tyrosine to 3-nitrotyrosine has profound consequences in terms of immunological reactivity (*17*).

Purification of nitrated peptides prior to MALDI-TOF analysis is an important step in fully characterizing tyrosine nitration sites. The presence of unmodified peptides significantly weakened the ability to detect and measure cytochrome *c* nitrated species by MALDI-TOF, in agreement with the notion proposed in ref *42*. In addition, the use of purified and well-characterized mononitrated cytochrome *c* species provides a tool for precisely studying the influence of tyrosine nitration at specific sites in cytochrome *c* function. Finally, the identification of cytochrome *c* nitration site(s) in vivo may assist in unraveling the chemical nature of proximal reactive nitrogen species.

[3] It is important to point out that mitochondrial oxygen consumption values of near 100% can be supported with only a fractional amount of the normal native cytochrome *c* content (*43*). Thus, slower respiration with respect to controls when replenishing cytochrome *c*-depleted preparations with nitrocytochrome *c* can be seen only if the "loss of function" of the modified cytochromes is large, e.g., >70−80%.

ACKNOWLEDGMENT

We thank Dr. Francisco J. Schopfer for helpful discussions and assistance with the artwork.

REFERENCES

1. Margoliash, E., and Schejter, A. (1996) in *Cytochrome c. A multidisciplinary approach* (Mauk, A., Ed.) pp 3−31, University Science Books, Sausalito, CA.
2. Jiang, X., and Wang, X. (2004) Cytochrome C-mediated apoptosis, *Annu. Rev. Biochem. 73*, 87−106.
3. Nantes, I. L., Zucchi, M. R., Nascimento, O. R., and Faljoni-Alario, A. (2001) Effect of heme iron valence state on the conformation of cytochrome *c* and its association with membrane interfaces. A CD and EPR investigation, *J. Biol. Chem. 276*, 153−158.
4. Kluck, R. M., Ellerby, L. M., Ellerby, H. M., Naiem, S., Yaffe, M. P., Margoliash, E., Bredesen, D., Mauk, A. G., Sherman, F., and Newmeyer, D. D. (2000) Determinants of cytochrome *c* pro-apoptotic activity. The role of lysine 72 trimethylation, *J. Biol. Chem. 275*, 16127−16133.
5. Pollock, W. B., Rosell, F. I., Twitchett, M. B., Dumont, M. E., and Mauk, A. G. (1998) Bacterial expression of a mitochondrial cytochrome *c*. Trimethylation of Lys72 in yeast iso-1-cytochrome *c* and the alkaline conformational transition, *Biochemistry 37*, 6124−6131.
6. Sokolovsky, M., Aviram, I., and Schejter, A. (1970) Nitrocytochrome *c*. I. Structure and enzymic properties, *Biochemistry 9*, 5113−5118.
7. Cassina, A. M., Hodara, R., Souza, J. M., Thomson, L., Castro, L., Ischiropoulos, H., Freeman, B. A., and Radi, R. (2000) Cytochrome *c* nitration by peroxynitrite, *J. Biol. Chem. 275*, 21409−21415.
8. Radi, R., Cassina, A., Hodara, R., Quijano, C., and Castro, L. (2002) Peroxynitrite reactions and formation in mitochondria, *Free Radical Biol. Med. 33*, 1451−1464.
9. Radi, R., Denicola, A., Alvarez, B., Ferrer, G., and Rubbo, H. (2000) in *Nitric Oxide Biology and Pathobiology* (Ignarro, L. J., Ed.) pp 57−82, Academic Press, San Diego.
10. Radi, R., Peluffo, G., Alvarez, M. N., Naviliat, M., and Cayota, A. (2001) Unraveling peroxynitrite formation in biological systems, *Free Radical Biol. Med. 30*, 463−488.
11. Eiserich, J. P., Hristova, M., Cross, C. E., Jones, A. D., Freeman, B. A., Halliwell, B., and van der Vliet, A. (1998) Formation of nitric oxide-derived inflammatory oxidants by myeloperoxidase in neutrophils, *Nature 391*, 393−397.
12. Creighton, T. E. (1993) *Proteins: Structures and Molecular Properties*, 2nd ed., W. H. Freeman and Company, New York.
13. MacMillan-Crow, L. A., Crow, J. P., Kerby, J. D., Beckman, J. S., and Thompson, J. A. (1996) Nitration and inactivation of manganese superoxide dismutase in chronic rejection of human renal allografts, *Proc. Natl. Acad. Sci. U.S.A. 93*, 11853−11858.
14. Guo, W., Adachi, T., Matsui, R., Xu, S., Jiang, B., Zou, M. H., Kirber, M., Lieberthal, W., and Cohen, R. A. (2003) Quantitative assessment of tyrosine nitration of manganese superoxide dismutase in angiotensin II-infused rat kidney, *Am. J. Physiol. 285*, H1396−H1403.
15. Radi, R. (2004) Nitric oxide, oxidants, and protein tyrosine nitration, *Proc. Natl. Acad. Sci. U.S.A. 101*, 4003−4008.
16. Vadseth, C., Souza, J. M., Thomson, L., Seagraves, A., Nagaswami, C., Scheiner, T., Torbet, J., Vilaire, G., Bennett, J. S., Murciano, J. C., Muzykantov, V., Penn, M. S., Hazen, S. L., Weisel, J. W., and Ischiropoulos, H. (2004) Pro-thrombotic state induced by post-translational modification of fibrinogen by reactive nitrogen species, *J. Biol. Chem. 279*, 8820−8826.
17. Birnboim, H. C., Lemay, A. M., Lam, D. K., Goldstein, R., and Webb, J. R. (2003) Cutting edge: MHC class II-restricted peptides containing the inflammation-associated marker 3-nitrotyrosine

evade central tolerance and elicit a robust cell-mediated immune response, *J. Immunol. 171*, 528−532.
18. Vanneste, W. H. (1966) Molecular proportion of the fixed cytochrome components of the respiratory chain of Keilin-Hartree particles and beef heart mitochondria, *Biochim. Biophys. Acta 113*, 175−178.
19. Thomson, L., Trujillo, M., Telleri, R., and Radi, R. (1995) Kinetics of cytochrome c^{2+} oxidation by peroxynitrite: Implications for superoxide measurements in nitric oxide-producing biological systems, *Arch. Biochem. Biophys. 319*, 491−497.
20. Castro, L., Eiserich, J. P., Sweeney, S., Radi, R., and Freeman, B. A. (2004) Cytochrome *c*: A catalyst and target of nitrite-hydrogen peroxide-dependent protein nitration, *Arch. Biochem. Biophys. 421*, 99−107.
21. Chen, Y. R., Chen, C. L., Chen, W., Zweier, J. L., Augusto, O., Radi, R., and Mason, R. P. (2004) Formation of protein tyrosine ortho-semiquinone radical and nitrotyrosine from cytochrome *c*-derived tyrosyl radical, *J. Biol. Chem. 279*, 18054−18062.
22. Borutaite, V., Morkuniene, R., and Brown, G. C. (1999) Release of cytochrome *c* from heart mitochondria is induced by high Ca^{2+} and peroxynitrite and is responsible for Ca^{2+}-induced inhibition of substrate oxidation, *Biochim. Biophys. Acta 1453*, 41−48.
23. Hortelano, S., Alvarez, A. M., and Bosca, L. (1999) Nitric oxide induces tyrosine nitration and release of cytochrome *c* preceding an increase of mitochondrial transmembrane potential in macrophages, *FASEB J. 13*, 2311−2317.
24. MacMillan-Crow, L. A., Cruthirds, D. L., Ahki, K. M., Sanders, P. W., and Thompson, J. A. (2001) Mitochondrial tyrosine nitration precedes chronic allograft nephropathy, *Free Radical Biol. Med. 31*, 1603−1608.
25. Schejter, A., Aviram, I., and Sokolovsky, M. (1970) Nitrocytochrome *c*. II. Spectroscopic properties and chemical reactivity, *Biochemistry 9*, 5118−5122.
26. Margoliash, E., and Lustgarten, J. (1962) Interconversion of horse heart cytochrome c monomer and polymers, *J. Biol. Chem. 237*, 3397−3405.
27. Brito, C., Naviliat, M., Tiscornia, A. C., Vuillier, F., Gualco, G., Dighiero, G., Radi, R., and Cayota, A. M. (1999) Peroxynitrite inhibits T lymphocyte activation and proliferation by promoting impairment of tyrosine phosphorylation and peroxynitrite-driven apoptotic death, *J. Immunol. 162*, 3356−3366.
28. Radi, R., Beckman, J. S., Bush, K. M., and Freeman, B. A. (1991) Peroxynitrite oxidation of sulfhydryls. The cytotoxic potential of superoxide and nitric oxide, *J. Biol. Chem. 266*, 4244−4250.
29. Trostchansky, A., Batthyany, C., Botti, H., Radi, R., Denicola, A., and Rubbo, H. (2001) Formation of Lipid−Protein Adducts in Low-Density Lipoprotein by Fluxes of Peroxynitrite and Its Inhibition by Nitric Oxide, *Arch. Biochem. Biophys. 395*, 225−232.
30. Radi, R., Thomson, L., Rubbo, H., and Prodanov, E. (1991) Cytochrome *c*-catalyzed oxidation of organic molecules by hydrogen peroxide, *Arch. Biochem. Biophys. 288*, 112−117.
31. Smith, P. K., Krohn, R. I., Hermanson, G. T., Mallia, A. K., Gartner, F. H., Provenzano, M. D., Fujimoto, E. K., Goeke, N. M., Olson, B. J., and Klenk, D. C. (1985) Measurement of protein using bicinchoninic acid, *Anal. Biochem. 150*, 76−85.
32. Margoliash, E., and Frohwirt, N. (1959) Spectrum of horse-heart cytochrome *c*, *Biochem. J. 71*, 570−572.
33. Sarver, A., Scheffler, N. K., Shetlar, M. D., and Gibson, B. W. (2001) Analysis of peptides and proteins containing nitrotyrosine by matrix-assisted laser desorption/ionization mass spectrometry, *J. Am. Soc. Mass Spectrom. 12*, 439−448.
34. Ischiropoulos, H., Zhu, L., Chen, J., Tsai, M., Martin, J. C., Smith, C. D., and Beckman, J. S. (1992) Peroxynitrite-mediated tyrosine nitration catalyzed by superoxide dismutase, *Arch. Biochem. Biophys. 298*, 431−437.
35. Alvarez, B., Rubbo, H., Kirk, M., Barnes, S., Freeman, B. A., and Radi, R. (1996) Peroxynitrite-dependent tryptophan nitration, *Chem. Res. Toxicol. 9*, 390−396.
36. Luntz, T. L., Schejter, A., Garber, E. A., and Margoliash, E. (1989) Structural significance of an internal water molecule studied by site-directed mutagenesis of tyrosine-67 in rat cytochrome *c*, *Proc. Natl. Acad. Sci. U.S.A. 86*, 3524−3528.
37. Dickerson, R. E., and Timkovich, R. (1975) in *The Enzymes* (Boyer, P., Ed.) pp 397−547, Academic Press, New York.
38. Souza, J. M., Daikhin, E., Yudkoff, M., Raman, C. S., and Ischiropoulos, H. (1999) Factors determining the selectivity of protein tyrosine nitration, *Arch. Biochem. Biophys. 371*, 169−178.
39. Prutz, W. A., Butler, J., and Land, E. J. (1985) Methionyl→tyrosyl radical transitions initiated by Br^{2-} in peptide model systems and ribonuclease A, *Int. J. Radiat. Biol. Relat. Stud. Phys., Chem. Med. 47*, 149−156.
40. Souza, J. M., Choi, I., Chen, Q., Weisse, M., Daikhin, E., Yudkoff, M., Obin, M., Ara, J., Horwitz, J., and Ischiropoulos, H. (2000) Proteolytic degradation of tyrosine nitrated proteins, *Arch. Biochem. Biophys. 380*, 360−366.
41. Chen, Y. R., Sturgeon, B. E., Gunther, M. R., and Mason, R. P. (1999) Electron spin resonance investigation of the cyanyl and azidyl radical formation by cytochrome *c* oxidase, *J. Biol. Chem. 274*, 24611−24616.
42. Petersson, A. S., Steen, H., Kalume, D. E., Caidahl, K., and Roepstorff, P. (2001) Investigation of tyrosine nitration in proteins by mass spectrometry, *J. Mass Spectrom. 36*, 616−625.
43. Turrens, J. F., Alexandre, A., and Lehninger, A. L. (1985) Ubisemiquinone is the electron donor for superoxide formation by complex III of heart mitochondria, *Arch. Biochem. Biophys. 237*, 408−414.

BI0474620